34th Annual International Conference of the IEEE EMBS
San Diego, California USA, 28 August - 1 September, 2012

Spherical Finite Rate of Innovation Theory for the Recovery of Fiber Orientations

Samuel Deslauriers-Gauthier, *Student Member, IEEE*, Pina Marziliano, *Member, IEEE*

***Abstract*— In this paper, we investigate the reconstruction of a signal defined as the sum of *K* orientations from samples taken with a kernel defined on the 3D rotation group. A potential application is the recovery of fiber orientations in diffusion magnetic resonance imaging. We propose an exact reconstruction algorithm based on the finite rate of innovation theory that makes use of the spherical harmonics representation of the signal. The number of measurements needed for perfect recovery, which may be as low as $3K$, depends only on the number of orientations and the bandwidth of the kernel used. Furthermore, the angular resolution of our method does not depend on the number of available measurements. We illustrate the performance of the algorithm using several simulations.**

I. Introduction

We consider a function f on the unit sphere in three dimension defined as the sum of K weighted Diracs such that

$$f(\theta,\varphi)=\sum_{k=1}^{K} a_k \delta(\theta-\theta_k,\varphi-\varphi_k)$$

where $0\le\varphi,\varphi_k<2\pi, 0\le\theta,\theta_k<\pi$ and each couple (θ_k,φ_k) corresponds to one orientation. The function to sample

$$s(\theta,\varphi)=(f*h)(\theta,\varphi)$$

is obtained by convolving f with a sampling kernel h defined on the 3D rotation group and where the convolution $*$ has been appropriately redefined. Our objective is to recover f from as few measurements of s as possible.

A notable application is the recovery of fiber orientation in diffusion weighted magnetic resonance imaging (MRI). In this case, f is the fiber orientation distribution function (ODF) and h is the response of a single fiber [1]. The typical way to recover the fiber ODF is to perform a spherical deconvolution [2]. However, because of the limited number of measurements available in diffusion MRI, only a lowpass version of the fiber ODF can be recovered. This is a limit common to other methods [3, 4, 5], where the angular resolution is a function of the number of measurements. Our proposed method improves this situation because the angular resolution is completely independent of the number of measurements. Note that we address the general problem of recovering f from the samples of s, thus we will not consider the specific characteristics of diffusion MRI signals, i.e. , f, and h are not necessarily real, positive, and symmetric. Due to space limitations, we will also restrict our discussion to noiseless measurements.

The remainder of this paper is organized as follows. In Section II, we provide the essential background information on spherical and rotational harmonics, and spherical deconvolution. In Section III, we present our new reconstruction algorithm along with specific requirements of the sampling kernel. We illustrate the performance of the algorithm in Section IV through numerical simulations and conclude in Section V.

The authors are with the School of Electrical and Electronic Engineering at the Nanyang Technological University, Singapore e-mail: {desl0001@e., epina@}ntu.edu.sg).

S. Deslauriers-Gauthier is funded by the Singapore International Graduate Award of the Agency for Science, Technology and Research (A*STAR), Singapore.

II. Spherical and rotational harmonics

In this section, we present a brief outline of Fourier analysis on the sphere S^2 and the group of all 3×3 real orthogonal matrices with a determinant of one is denoted by $SO(3)$. We restrict our discussion to the definitions and properties that will be used in the following sections. For a more detailed analysis, we refer the reader to [2, 6].

A. Rotational harmonics

Let $g\in SO(3)$ be a 3×3 rotation matrix that can be expressed as

$$g(\phi,\theta,\varphi)=\alpha(\phi)\beta(\theta)\alpha(\varphi)$$

where

$$\alpha(x)=\begin{bmatrix}\cos x & -\sin x & 0\\ \sin x & \cos x & 0\\ 0 & 0 & 1\end{bmatrix}, \beta(x)=\begin{bmatrix}\cos x & 0 & \sin x\\ 0 & 1 & 0\\ -\sin x & 0 & \cos x\end{bmatrix},$$

and $0\le\phi,\varphi<2\pi, 0\le\theta<\pi$. Healy *et al.* [2] define the rotational Fourier transform on $SO(3)$ as

$$\hat{h}_\ell^{mn}=\int_{SO(3)} h(g)D_\ell^{mn}(g)\,dg$$

with $\ell=0,\dots,\infty$ and $-\ell\le m,n\le\ell$. The rotational harmonics D_ℓ^{mn} are given by

$$D_\ell^{mn}\big(g(\phi,\theta,\varphi)\big)=j^{m-n}\exp(-jm\phi)d_\ell^{mn}(\theta)\exp(-jn\varphi)$$

where

$$d_\ell^{mn}(\theta)=\frac{(\sin^{n-m}\theta)(1+\cos\theta)^m}{s^\ell[(\ell+m)!\,(\ell-m)!]^{1/2}}\left[\frac{(\ell-n)!}{(\ell+n)!}\right]^{1/2}\times\frac{d^{\ell+n}}{d(\cos\theta)^{\ell+n}}(\cos\theta-1)^{\ell+m}(1+\cos\theta)^{\ell-m}.$$

B. Spherical harmonics

The spherical harmonic of degree ℓ and order m is defined as

$$Y_\ell^m(\theta,\varphi) = N_{\ell m} P_\ell^m(\cos\theta)\exp(jm\varphi) \quad (1)$$

where $N_{\ell m}$ is a normalization coefficient,

$$P_\ell^m(\cos\theta) = (-1)^m \sin^m\theta \frac{d^m}{d(\cos\theta)^m} P_\ell(\cos\theta)$$

and

$$P_\ell(x) = \frac{1}{2^\ell \ell!}\frac{d^\ell}{dx^\ell}(x^2-1)^\ell.$$

Now consider the square integrable function $f(\theta,\varphi) \in L^2(S^2)$. It is sometimes more convenient to express f as a function of a unit vector ω related to (θ,φ) by

$$\omega(\theta,\varphi) = [\cos\varphi\sin\theta \quad \sin\varphi\sin\theta \quad \cos\theta]^t \quad (2)$$

where $\cdot^t$ denotes transposition. To simplify the notation, we will interchangeably write $f(\omega)$ and $f(\theta,\varphi)$ where we assume that both functions are equal if θ,φ, and ω are related by Eq. (2). Healy *et al.* define the spherical Fourier transform on S^2 by

$$\hat{f}_\ell^m = \int_{S^2} f(\omega)\overline{Y_\ell^m}(\omega)d\omega$$

where the overbar denotes conjugation and the $\hat{f}_\ell^m$ are the spherical harmonic coefficients. Because the spherical harmonics Y_ℓ^m for $\ell = 0,\dots,\infty$ and $-\ell \le m \le \ell$ form an orthonormal basis for $L^2(S^2)$, any $f \in L^2(S^2)$ can be expressed as

$$f(\theta,\varphi) = \sum_{\ell=0}^{\infty}\sum_{m=-\ell}^{\ell} \hat{f}_\ell^m Y_\ell^m(\theta,\varphi). \quad (3)$$

C. Spherical convolution

Let $f \in L^2(S^2)$ and $h \in L^2(SO(3))$ and define $s \in L^2(S^2)$ as the spherical convolution of f and h given by

$$s(\omega) = (f*h)(\omega) = \int_{SO(3)} h(g)f(g^{-1}\omega)dg. \quad (4)$$

The results of Healy *et al.* [2] prove the spherical convolution property

$$\hat{s}_\ell^m = \widehat{(f*h)}_\ell^m = \sum_{n=-\ell}^{\ell} \hat{f}_\ell^n \hat{h}_\ell^{mn} \quad (5)$$

for each $\ell = 0,\dots,\infty$ and any $-\ell \le m \le \ell$. An important relationship between the spherical and rotational harmonics, used to prove the convolution property, is that

$$Y_\ell^m(g\omega) = \sum_{i=-\ell}^{\ell} Y_\ell^i(\omega)\, D_\ell^{im}(g^{-1}). \quad (6)$$

III. Sampling orientations

As stated in the Introduction, the function to sample is given by

$$s(\omega) = (f*h)(\omega)$$

where $h \in L^2(SO(3))$ is the sampling kernel and

$$f(\theta,\varphi) = \sum_{k=1}^{K} a_k \delta(\theta-\theta_k, \varphi-\varphi_k) \quad (7)$$

with $a_k \in \mathbb{R}$, $0 \le \theta,\theta_k \le \pi$ and $0 \le \varphi,\varphi_k \le 2\pi$. Note that the function f is completely defined by $3K$ parameters; the K orientations (θ_k,φ_k) and the K amplitudes a_k.

Our objective is to recover f exactly from as few measurements of s as possible given the knowledge of K and h. The reconstruction algorithm has two major steps:

1. Recover the spherical harmonics of f using the samples of s.
2. Using the spherical harmonics, recover the parameters θ_k, φ_k and a_k which fully define f.

The details of these two steps are presented in the following sections.

A. Recovering the spherical harmonics

We previously defined the signal measured in diffusion magnetic resonance imaging as

$$s(\theta,\varphi) = (h*f)(\omega) = \int_{SO(3)} h(g)f(g^{-1}\omega)dg.$$

Because the function f is defined on the two dimensional sphere S^2, we can substitute it by its spherical harmonics expansion defined in Eq. (3) to get

$$(h*f)(\omega) = \int_{SO(3)} h(g)\left(\sum_{\ell=0}^{\infty}\sum_{m=-\ell}^{\ell} \hat{f}_\ell^m Y_\ell^m(g^{-1}\omega)\right)dg.$$

To expand the spherical harmonics, we can use the relation of Eq. (6) and rearrange the order of the sum and the integral to get

$$(h*f)(\omega) = \sum_{\ell=0}^{\infty}\sum_{m=-\ell}^{\ell} \hat{f}_\ell^m \sum_{i=-\ell}^{\ell} Y_\ell^i \int_{SO(3)} h(g)D_\ell^{im}(g)dg.$$

Substituting the definition of the rotational Fourier transform yields

$$(h*f)(\omega) = \sum_{\ell=0}^{\infty}\sum_{m=-\ell}^{\ell} \hat{f}_\ell^m \hat{p}_\ell^m(\omega) \quad (8)$$

where

$$\hat{p}_\ell^m(\omega) = \sum_{i=-\ell}^{\ell} Y_\ell^i(\omega)\hat{h}_\ell^{im}.$$

If we assume the sampling kernel h has a bandlimit L, meaning $\hat{h}_\ell^{im} = 0$ for $\ell > L$, Eq. (8) and hence the measured signal can be expressed as

(a) (b) (c) (d)

Figure 1: Illustration of the performance of the reconstruction algorithm for 2 orientations. The separation angles are 90 (a), 60 (b), 30 (c) and 10 (d) degrees. In all cases, the orientations are recovered to machine precision.

$$s(\omega) = \sum_{\ell=0}^{L} \sum_{m=-\ell}^{\ell} \hat{f}_\ell^m \, \hat{p}_\ell^m(\omega) \tag{9}$$

which requires $\sum_{\ell=0}^{L}(2\ell+1)$ values of s to solve for $\hat{f}_\ell^m$. If we have complete control over h, the number of measurements required can be reduced to $3K$ by setting all superfluous $\hat{h}_\ell^{mn}$ to zero.

Now that the spherical harmonics of f can be recovered from the samples of s, we move on to recovering the orientation from the spherical harmonics.

B. Recovering the orientations

Recall the definition of the spherical harmonics

$$\hat{f}_\ell^m = \int_{S^2} f(\omega)\overline{Y_\ell^m}(\omega)d\omega$$

and replace f by the stream of Diracs defined in Eq. (7) to get

$$\hat{f}_\ell^m = \sum_{k=1}^{K} a_k \overline{Y_\ell^m}(\theta_k, \varphi_k) \tag{10}$$

where we used the sifting property of the Diracs. Substituting the definition of the spherical harmonics in Eq. (10) yields

$$\hat{f}_\ell^m = N_\ell^m \sum_{k=1}^{K} a_k e^{-jm\varphi_k} P_\ell^m(\cos\theta_k). \tag{11}$$

We first consider the associated Legendre polynomials of equal order and degree $P_n^n(\cos\theta)$ given by

$$P_n^n(\cos\theta) = N_n \sin^n\theta$$

where N_n is a normalization coefficient. Replacing $P_n^n(\cos\theta)$ in Eq. (11) gives

$$\hat{f}_n^n = N_{nn}N_n \sum_{k=1}^{K} a_k e^{-jn\varphi_k} \sin^n\theta_k. \tag{12}$$

Using the notation $u_k = e^{-j\varphi_k}$, $s_k = \sin\theta_k$, $r_k = u_k s_k$, and $z_n = \hat{f}_n^n/(N_{nn}N_n)$ we can reduce Eq. (12) to

$$z_n = \sum_{k=1}^{K} a_k r_k^n. \tag{13}$$

The readers familiar with finite rate of innovation signals [7, 8] will immediately recognize the sum of exponential form and conclude that a_k and r_k can be recovered using the annihilating filter method. We briefly outline the recovery procedure here.

Consider the polynomial of degree K given

$$h(x) = \prod_{k=1}^{K}(x - r_k^{-1})$$

whose roots are r_k^{-1}, where $k = 1, \dots, K$. The convolution between the filter whose coefficients are $h_1, \dots, h_{K+1}$ and the z_n is

$$\sum_{i=0}^{K} h_i z_{n-i} = \sum_{i=0}^{K} h_i \left(N \sum_{k=1}^{K} a_k r_k^{n-i} \right)$$
$$= N \sum_{k=1}^{K} a_k r_k^n \underbrace{\sum_{i=0}^{K} h_i r_k^{-i}}_{h(r_k^{-1})=0} = 0.$$

We conclude that the roots of the annihilating filter h uniquely define the values r_k with $k = 1, \dots, K$. Note that $r_k = s_k u_k$ where u_k is a complex exponential and $s_k = \sin\theta_k$ is a real number in the interval $[0,1]$. In other words, φ_k and s_k correspond to the phase and magnitude of r_k, respectively. Unfortunately, the angle $\theta_k \in [0, \pi]$ cannot be obtained directly from s_k because two values of θ_k map to the same s_k. However, now that we know the values r_k, the quantity a_k can be recovered by solving

$$z_n = \sum_{k=1}^{K} a_k r_k^n$$

for $n = 0, \dots, K-1$.

To disambiguate the values of θ_k, we turn to the associated Legendre polynomials

$$P_n^{n-1} = -N_n \cos\theta \sin^{n-1}\theta$$

and their associated spherical harmonics

$$\hat{f}_n^{n-1} = -N_{nn}N_n \sum_{k=1}^{K} a_k e^{-jn\varphi_k} \sin^{n-1}\theta_k \cos\theta_k.$$

Again simplifying the notation with $c_k = \cos\theta_k$ and $w_n = -\hat{f}_n^{n-1}/(N_{nn}N_n)$ we find that

$$w_n = \sum_{k=1}^{K} a_k c_k r_k^{n-1}. \tag{14}$$

All the coefficients in the Eq. (14) are known except for c_k which can be recovered using w_n for $n = 1, \dots, K$. Because

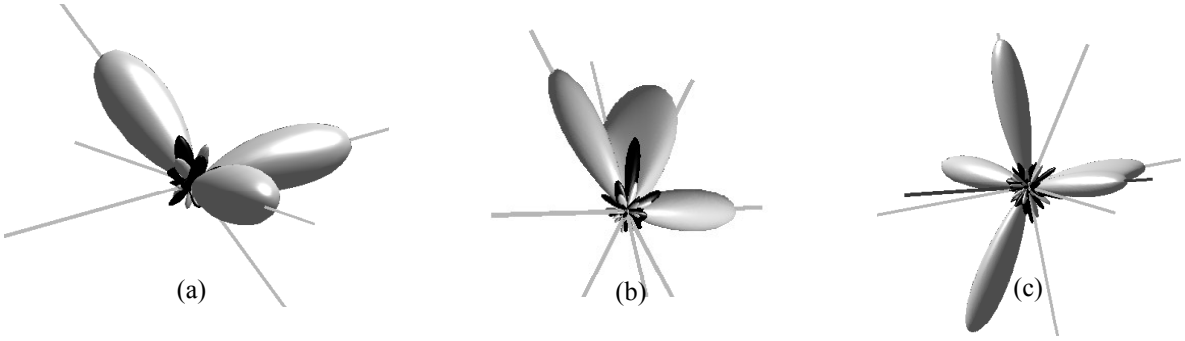

Figure 2: Illustration of the performance of the reconstruction algorithm for (a) $K = 3$, (b) $K = 4$, and (c) $K = 5$ orientations.

$\cos\theta$ has a one-to-one correspondence in the interval $[0, \pi]$ the value of c_k uniquely defines the angle θ_k.

IV. Numerical simulations

To evaluate the reconstruction algorithm presented in the previous section, we performed several simulations with $K = 2$, 3, 4, and 5. Without loss of generality, we considered only the sampling kernel whose rotational harmonics are

$$\hat{h}_\ell^{mn} = \begin{cases} 1 & \ell \le L \\ 0 & \text{otherwise} \end{cases}$$

with $L = 2K$. Note that this kernel is suboptimal if we wish to minimize the number of measurements required.

Given K and a sampling kernel h with a bandwidth L, the artificial data is generated as follows:

1. Randomly select the values for θ_k, φ_k, and a_k with $k = 1, \dots, K$.
2. Compute the spherical harmonics of f using Eq. (11).
3. Compute the spherical harmonics of s using to Eq. (5).
4. Generate the samples at the desired location $\omega_1, \dots, \omega_N$ using

$$s(\omega) = \sum_{\ell=0}^{L} \sum_{m=-\ell}^{\ell} \hat{s}_\ell^m Y_\ell^m(\omega).$$

We assume the number of fibers K is known a priori and that the number of samples is sufficient to compute $\hat{f}_\ell^m$ from Eq. (9). Since the location of the samples is irrelevant, we selected them at random on the north half-sphere.

For the case $K = 2$, we tested separation angles varying from 10 to 90 degrees. In all cases, the orientations were recovered to machine precision. Sample results for separation angles of $10, 30, 60,$ and 90 are illustrated in Figure 1. The radius in a direction corresponds to the magnitude of the real component of the signal in that direction. Positive and negative values are displayed in gray and black, respectively. The solid lines represent the orientations.

TABLE I. Mean angular error as a function of K over 100 simulations

	$K = 2$	$K = 3$	$K = 4$	$K = 5$
Error (deg)	0.0000	0.0006	0.3273	2.3745

We also tested 100 random generated orientations for each $K = 2, 3, 4,$ and 5 (in diffusion MRI, the number of fibers in a voxel is generally assumed to be less than or equal to 3). The mean angular error is presented in Table I. Sample results for each value of K are illustrated in Figure 2. The angular error is negligible for $K \le 3$ and increases with K, probably due to numerical errors.

V. Conclusion

In this work, we have presented a new algorithm to recover orientations on the unit sphere in three dimensions. In the noiseless case, the proposed method is exact if the bandwidth of the kernel satisfies $L \ge 2K$ and that the number of measurements satisfies $N \le \sum_{\ell=0}^{L}(2\ell + 1)$. When compared to other spherical deconvolution, our method is advantageous because the angular resolution does not depend on the number of measurements available. Investigating the robustness of our method to additive noise and applying it to diffusion MRI is the subject of our current research.

References

[1] J. Donald Tournier, Fernando Calamante, David G. Gadian and Alan Connelly, *Direct estimation of the fiber orientation density function from diffusion-weighted MRI data using spherical deconvolution*, NeuroImage, pp. 1176-1185, 2004.

[2] Dennis M. Healy, Harrie Hendriks and Peter T. Kim, *Spherical deconvolution*, Journal of Multivariate Analysis, pp. 1-22, 1998.

[3] Maxime Descoteaux, Elaine Angelino, Shaun Fitzgibbons and David Deriche, *Regularized, fast, and robust analytical Q-ball imaging*, Magnetic Resonance in Medicine, pp. 497-510, 2007.

[4] Van J. Wedeen, Patric Hagmann, Wen-Yih Isaac Tseng, Timothy G. Reese and Robert M. Weisskoff, *Mapping complex tissue architecture with diffusion spectrum magnetic resonance imaging*, Magnetic Resonance in Medicine, pp. 1377-1386, 2005.

[5] Fang-Cheng Yeh, Van Jay Wedeen and Weh Yih Isaac Tseng, *Generalized q-sampling imaging*, IEEE Transactions on Medical Imaging, pp. 1626-1635, 2010.

[6] James Ting-Ho Lo and Linda R. Eshleman, *Exponential Fourier densities on SO(3) and optimal estimation and detection for rotational processes*, Society for Industrial and Applied Mathematics, pp. 73-82, 1979.

[7] Thierry Blu, Pier Luigi Dragotti, Martin Vetterli, Pina Marziliano and Lionel Coulot, *Sparse sampling of signal innovations*, IEEE Signal Processing Magazine, pp. 31-40, 2008.

[8] Martin Vetterli, Pina Marziliano and Thierry Blu, *Sampling signals with finite rate of innovation*, IEEE Transactions on Signal Processing, pp. 1417-1428, 2002.